INVESTIGATION OF THE FLUIDISED ZONE IN DEEP VIBROCOMPACTION

Moritz Wotzlaw*, *Technische Universität Berlin, Chair of Soil Mechanics and Geotechnical Engineering, moritz.wotzlaw@tu-berlin.de*

ABSTRACT

Deep vibrocompaction is an established method for the improvement of loose sandy soils using deep vibrators. In a basic modelling concept, the area of the ground influenced by the vibrator is subdivided into three concentric cylindrical zones. According to that model, the compaction occurs only in some distance to the vibrator, since the acceleration amplitudes in the vicinity, the so-called fluidised zone, are considered too large. *Fluidisation* is defined and distinguished from *liquefaction*. Both phenomena can occur in the vicinity of the vibrator and so both have to be adequately considered in a simulation. A numerical model is developed and verified, while locally undrained conditions are applied in order to simulate liquefaction. Since mesh distortion becomes excessive, an MMALE-approach is being used.

Keywords: Soil Improvement, Vibroflotation, Numerical Modelling, MMALE, Large Deformations, Fluidisation, Liquefaction

1. INTRODUCTION

Since its invention by the German company Keller in the 1930s, deep vibrocompaction has become a widely used method for soil improvement [1]. The vibrator basically consists of a steel tube of about 3 m length, in which a rotating imbalance creates a centrifugal force causing a circular movement with a conoidal envelope (Fig. 1). It is connected to an extension tube via a joint and can be lowered to depths of up to 40 m. A basic modelling concept consists in subdividing the soil influenced by the vibrator into three concentric cylindrical zones (Fig. 2): Fluidised zone (A), compaction zone (B) and elastic zone (C).

First 2D attempts at modelling vibrocompaction numerically were carried out by [2], followed by [3] and [4]. More recently, full 3D-Simulations using the Coupled-Eulerian-Lagrangian (CEL) method (e.g. [5], [6]) were conducted, which seem to be rather unsuitable for a practical use due to the computational time necessary and the inability of the incremental constitutive law to correctly predict accumulated strains after a large number of cycles.

A more convenient solution is expected from a method, that has already been applied to vibratory pile driving ([7], [8]). In this two-step-scheme, a hypoplastic constitutive law [9] is used to determine the distribution of strain amplitudes, which then serve as the input data for the explicit calculation of accumulated plastic strains after 100s or even 1000s of cycles using the High Cycle Accumulation Model (HCA) [10].

A similar approach will be applied in this DFG-funded cooperation project of TUB, KIT and Keller Grundbau GmbH. While the authors task at TUB consists in the determination of strain amplitudes in the vicinity of the vibrator using Non-Lagrangian numerical methods, the researchers at the Karlsruher Institut für Technologie are involved in the enhancement of the HCA-Model for large strain amplitudes.

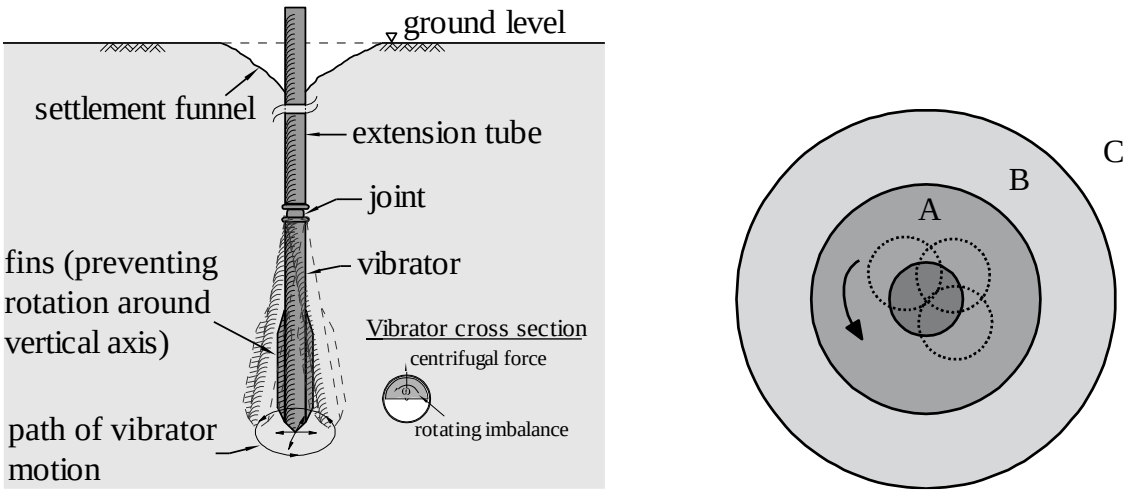

***Figure 1**. Schematic of deep vibrocompaction (left) and Modelling concept: fluidised zone (A), compaction zone (B) and elastic zone (C) (right, both after [1])*

In-situ data obtained at construction sites by Keller Grundbau GmbH will be used for validating the numerical results.

2. MODELLING THE SOIL BEHAVIOR

In this chapter the theoretical background for the soil mechanical processes is briefly introduced.

2.1. Constitutive Model

The constitutive model applied in the numerical FE-simulations with explicit time integration is the well-known Hypoplasticity with intergranular strains [9]. The existing implementation by Mašín [12] was incorporated into the LS-DYNA UMAT using an interface written by Bakroon et. al. [13].

2.2. Locally Undrained Conditions

Since vibrocompaction is often used in soils where groundwater is present, a consideration of porewater is necessary. As stated in [14], *locally undrained* conditions are obtained by neglecting the porewater flow in a water-saturated soil, which means that volumetric strain occurs only due to a compression of the pore fluid.

With the rate form of Terzaghi's principle of effective stress, the locally undrained approach can be implemented into any material stress-point routine by simply adding the porewater pressure to the effective stress tensor $\dot{\boldsymbol{\sigma}}'$, computed with the given constitutive law:

$$\dot{\boldsymbol{\sigma}} = \dot{\boldsymbol{\sigma}}' + \dot{p}\boldsymbol{I} \tag{1}$$

With

$$\dot{p} = \dot{\varepsilon}_{\mathrm{v}} \frac{K_{\mathrm{f}}}{n} \tag{2}$$

being the rate of porewater pressure, calculated from the rate of volumetric strain $\dot{\varepsilon}_{\mathrm{v}}$, the bulk modulus of the pore fluid K_{f} and the porosity n.

2.3. Liquefaction and Fluidisation

Two phenomena may strongly influence the soil behavior in Zone A and B: *Liquefaction* whenever pore water is present and *fluidisation* even if the soil is completely dry. While both of them are characterized by a decrease of shear strength and describe the fact that in this state the soil behaves like a viscous fluid, the mechanisms involved are not naturally the same.

Liquefaction is a rather well-understood phenomenon in a loose saturated granular soil under cyclic loading. The induced compactive grain rearrangement can't be directly transferred to a volumetric compression because of the present interstitial water and causes a decrease of effective stress and consequently of shear strength instead. Given that the total stress is constant, this leads to an increase of porewater pressure.

Fluidisation on the other hand is not well-established in the world of geotechnical engineering. It may be described as a reduction of shear strength and change of density caused by large acceleration amplitudes. Although it has been the subject of numerous experimental investigations in the past (an overview can be found in [16]) it has not yet been included in a constitutive law to be implemented into common numerical methods like the FEM. Besides the influence on shear strength it was found, that vertical vibrations with large accelerations cause dilation, while horizontally vibrations tend to compact the fluidised granular matter.

3. NUMERICAL MODEL

The current numerical model is a straightforward application of the modelling concept in Fig. 1. Since the essential soil mechanical processes are expected to occur in the horizontal plane, the soil is modelled as a pseudo-two-dimensional disc composed of 3D elements. According to [3] and [4] this is a justifiable compromise between full 3D- and oversimplified plane-strain-models.

3.1. Numerical Method

In the immediate vicinity of the vibrator, large soil deformations are expected. This is especially true, when the shear strength is decreased by liquefaction under undrained conditions. The application of numerical methods capable of handling large deformations is therefore necessary.

In a *Lagrange* formulation the material is fixed to the computational mesh and any material deformation causes mesh deformation. By contrast in a *Eulerian* formulation, the mesh is fixed in space and the material may move freely through it. ALE formulations combine the advantages of both views by introducing a reference domain, which is used to independently describe mesh and material motion [18].

In most numerical implementations, a three-step calculation scheme is applied, consisting of a Lagrange step (mesh deforms with material), rezoning step (mesh gets smoothed while the mesh topography is preserved) and advection step (the material "flows" relative to the rezoned mesh in order to retrieve the material state after the Lagrange step). ALE formulations are well suited for the application in geotechnical problems involving large deformations.

3.2. Geometry

The geometry is pictured in Fig. 2. For verification, the same geometry and model size as in [4] is being adopted. The disc has a radius of 15 m and a depth of 0.5 m. The inner hole containing the vibrator has a diameter of 0.4 m.

3.3. Soil Properties

The hypoplastic parameters for the soil in Tab. 1 are taken from [4] with an initial void ratio of 0.85. With a given grain density of 2.65 g/cm³, an initial dry density of 1.43 g/cm³ is obtained.

The initial stress state is taken as a K_0-state with $K_0 = 0.463$.

Table 1. *Parameters for Hypoplasticity with intergranular strains*

φ_c	h_s *in MPa*	n	e_{d0}	e_{c0}	e_{i0}	α	β	R	m_R	m_T	β_r	χ
32.5°	**591**	**0.5**	**0.577**	**0.874**	**1.005**	**0.12**	**1.0**	**10^{-4}**	**2.9**	**1.45**	**0.2**	**6.0**

3.4. Boundary Conditions

The soil disc is fixed in horizontal (x- and y-) directions. The horizontal boundary surfaces are provided with viscous boundaries following the approach of [15] for minimizing wave reflection.

Although the choice of the "correct" vertical boundaries is not obvious, for the sake of verifying the basic numerical model, pure stress boundaries are applied analogously to [4]. Since the modelled depth of the soil disc is 14.5 m to 15 m below ground level, the vertical stresses are given by $\sigma_{z,t} = 203\ kN/m^2$ at the top and $\sigma_{z,b} = 210\ kN/m^2$ at the bottom.

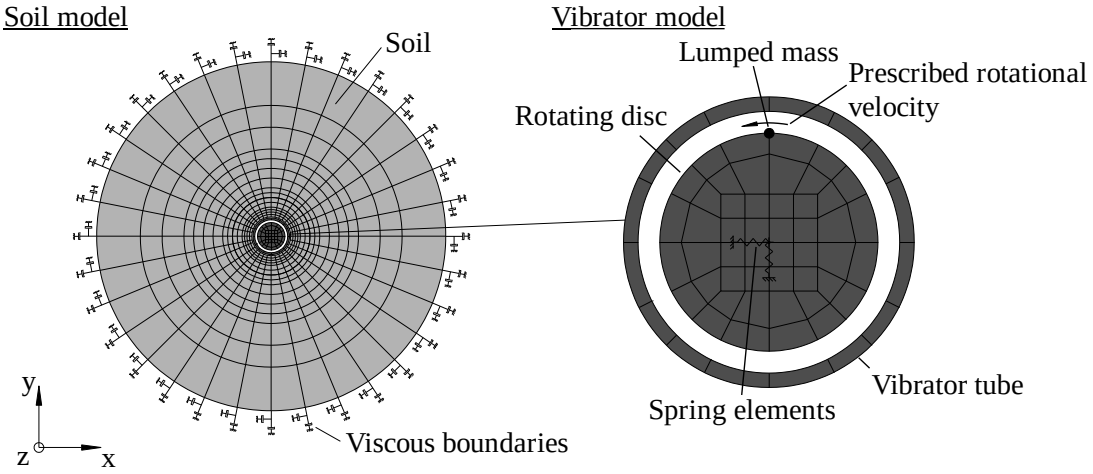

Figure 2*. Disc shaped soil model (left, top view) and vibrator model with rotating imbalance (right)*

3.5. Vibrator Model

For reproducing the in-plane movement of the vibrator as realistic as possible, it is modelled as a tube of rigid solid elements inside of which a lumped mass rotating on a disc composed of rigid shell elements causes a circular movement (Fig. 2, right). By coupling the translational DOFs from tube and the disc's middle node, this motion is transferred to the tube, reproducing the imbalance-driven motion of the vibrator.

Spring elements are attached to the vibrators center, restraining the movements to a circular path of a defined amplitude, which can be determined by the quotient of centrifugal force and spring stiffness.

With a centrifugal force of $F = 700\ kN$ and a spring stiffness of $k = 1 \cdot 10^5\ kN/m$ a displacement amplitude of $u_{vib} = 7\ mm$ (in the air) is obtained which is approximately the mean nodal displacement amplitude in [4].

Modelling the soil-vibrator interface is achieved via the use of a penalty contact algorithm.

4. NUMERICAL RESULTS

After verifying the Lagrange model, the influence of interface friction and the size of Zone A is discussed. Local undrained conditions are applied for modelling liquefaction.

4.1. Verification of Lagrange Model

For verifying the basic Lagrange model, it is compared to the results published in [4]. In their study, the authors applied circular nodal movements with a radius of 6.25 mm at the top and 7.5 mm at the bottom and a frequency of 30 Hz to the nodes at the inner boundary to simulate the vibrator impact. In a first step this vibrator model was adopted to test the models capability to reproduce the published results. The resulting void ratio distribution for the model verification (LS-DYNA with nodal movements vs. published results from [4]) is pictured in Fig. 3 on the left. It shows a fairly good agreement considering the fact, that the results were obtained using different FE-Codes and calculation schemes.

The results resemble the aforementioned 3-Zone-Model of Fig. 2: In the distance of more than ~5 m, the void ratio stays close to the initial value (Zone C). While the void ratio is reduced very fast in a distance between 0.5 and about 5 m (Zone B), it also remains at a rather high value in the region of <0.5 m distance from the vibrator (Zone A). This uncompacted zone is attributed to large shear strain amplitudes in [4]. Although that does explain the soil behavior in the hypoplastic model, it is not certain that this is also true in reality. Several authors (e.g. [19]) investigated the volumetric behavior of sand under cyclic large shear strain amplitudes and reported that, although the soil behaves dilatant during single cycles, the overall tendency is indeed compressive.

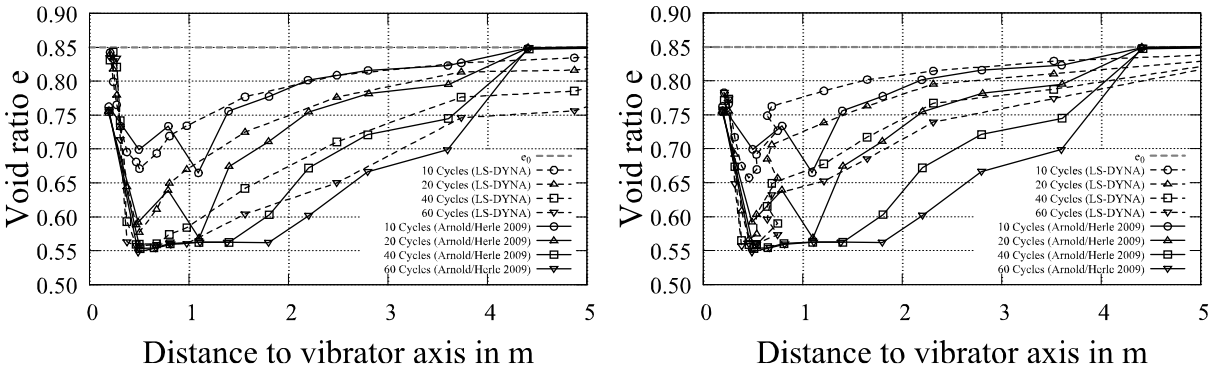

Figure 3*. Void ratio distribution with nodal movement model (left) and imbalance model (right). Dashed lines: results obtained with LS-DYNA, solid lines: results taken from [4]*

The diagram on the right-hand side of Fig. 3 shows the results obtained with the LS-DYNA imbalance model using a frictionless contact between vibrator and soil, compared to the results published in [4]. Although the results are similar in a qualitative way (formation of Zones A, B and C), a strong aberration is visible. This difference is mostly caused by the different assumptions for the soil-vibrator interface. In [4], the nodes in the contact surface move on a constant circular path so the radial and tangential amplitudes have the same size. This corresponds to a fully welded contact. In the imbalance model, the nodal movements are caused by the impact of the vibrator tube and since no friction was applied, only radial forces are transferred.

A very important input value for the latter simulations using the HCA-Model is the size of the fluidised zone. Following the initial model concept, one could consider the uncompacted region in the vicinity of the vibrator as fluidised, but as was pointed out before this doesn't fit the definition of fluidisation, since non-compactive behavior in the model is caused by large strain rather than large acceleration amplitudes.

The dimensionless amplitude of horizontal acceleration $\Gamma_h = a_h/g$ over a timestep of 0.4 s in different distances to the vibrator axis is given in fig 4. Following the suggestions in [1] the soil is considered fluidised for amplitudes between 1.5 and 3 g, so the fluidised zone would end in a distance of about 1.5 m to the vibrator axis. On the other hand, the reliability of this criterion is doubtful since the influence of a surcharge on the acceleration needed for fluidisation is present (as was pointed out by [16]) but not quantifiable, as no experimental results for large surcharges are available. In a more pragmatic approach for the following works, the outer boundary of zone A will be defined by the size of the largest strain amplitude ε_{ampl} that can be handled by the updated HCA-model.

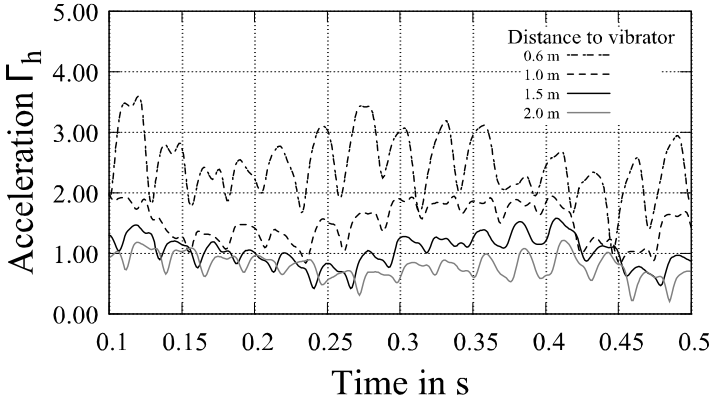

***Figure 4**. Acceleration amplitude Γ_h for different distances to vibrator (LS-DYNA imbalance model)*

4.2. Influence of Interface Friction

A comparison of void ratio distributions for the nodal displacements model and imbalance model with a friction coefficient of $\mu = 1.0$, both obtained with LS-DYNA, is given in Fig. 5. The agreement is much better than without friction, especially for rather few cycles.

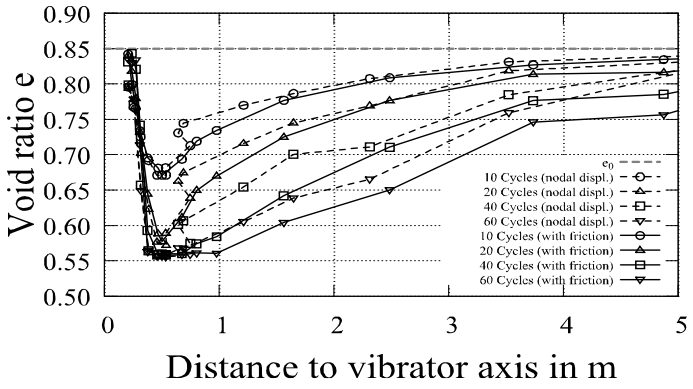

***Figure 5**. Void ratio distribution for LS-DYNA simulations using the nodal displacements model (dashed lines) and the imbalance model with friction coefficient of 1.0*

This directly leads to the conclusion, that applying an unrealistically high interface friction or even fully welded contact, may cause a severe overestimation of the compaction zone's extension. More attention should therefore be put to the determination of realistic interface properties.

4.3. Locally Undrained Conditions

In a next step the locally undrained approach is applied. Because of the large deformations due to the reduction of shear strength, the calculation aborts after a few cycles in the pure Lagrangian model, so an MMALE-approach is used on a smaller model at first, to keep the computational time at a reasonable level.

Fig. 6 shows the evolution of the effective mean pressure distribution over time. While it monotonically drops to a very small value (compared to the initial stress level) in an annular region with an inner radius of 0.5 m, it oscillates on a much higher stress level in the vicinity. This corresponds well to the observation stated in section 4.1. concerning the distribution of void ratio, since the increase/decrease of pore water pressure, just like the change of void ratio, depends on the volumetric strain, i.e. the liquefied zone under water saturated and undrained conditions is part of the compaction zone under dry conditions. A similar observation was stated already in [7] and attributed to the inability of the hypoplastic model to correctly model the liquefaction behavior under cyclic shearing with large amplitudes in [17]. The outer radius reaches a value of about 2 m rather fast and essentially doesn't grow any larger.

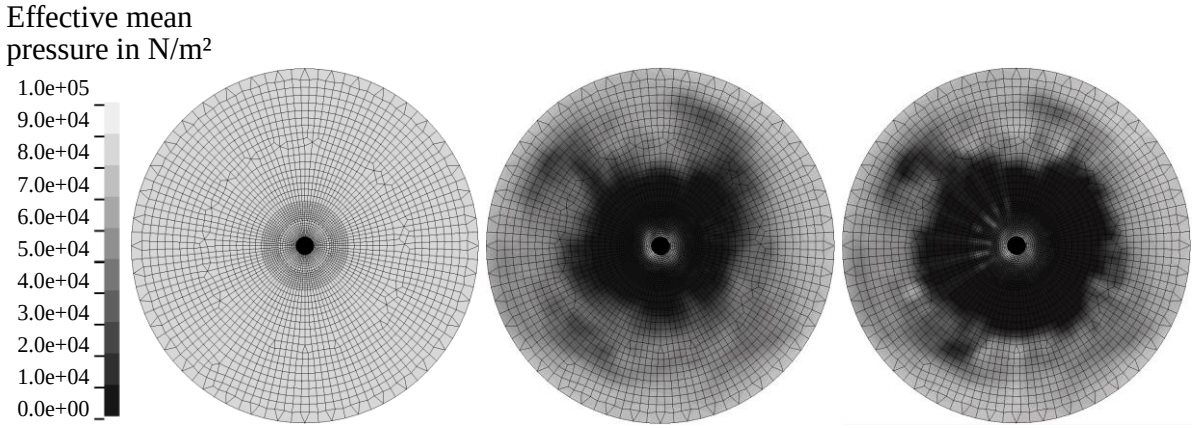

***Figure 6**. Distribution of effective mean pressure after 0 s, 0.1 s, 1 s*

5. CONCLUSION

Since a physically realistic description of the fluidised material is not possible with the existing tools, a pragmatic definition for Zone A has to be found based on the capability of the used constitutive law. It was shown that the interface friction between soil and vibrator plays a most important role and unrealistic high values may cause an overestimation of the compactions zone extent. The application of an MMALE approach to the current model seems to be unnecessary in the case of dry sand. When applying locally undrained conditions, the deformations become excessive due to the vanishing of shear strength in the liquefied soil and calculations fail using the Lagrange model, while an MMALE model is able to produce plausible results.

Future work has to account for viscous material behavior of the liquefied and/or fluidised soil, as well as porewater flow.

It is also of greatest importance, that experimental data is obtained in order to validate the simulation results. In fact, in-situ and laboratory tests are being carried out by different institutions, but at present results are not available.

ACKNOWLEDGEMENT

Funded by the Deutsche Forschungsgemeinschaft (German Research Foundation) – Projectnumber 341427400.

REFERENCES

[1] Kirsch, K., Kirsch, F., 2017. "*Ground Improvement by Deep Vibratory Methods*", Second Edition, CRC Press/Taylor & Francis Group, USA, 234 pages.

[2] Fellin, W., 2000. "*Rütteldruckverdichtung als plastodynamisches Problem*", Ph.D. Thesis, University of Innsbruck, Institute of Geotechnics and Tunnelling, Austria, 194 pages.

[3] Heibrock, G., Keßler, S., Triantafyllidis, T., 2006. "*On Modelling Vibro-Compaction of Dry Sands*", In: *Numerical Modelling of Construction Processes in Geotechnical Engineering for Urban Environment*, Edited by T. Triantafyllidis, Taylor & Francis Group plc, London, 125-132

[4] Arnold, M., Herle, I., 2009. "*Comparison of Vibrocompaction Methods by Numerical Simulations*", International Journal for Numerical and Analytical Methods in Geomechanics, 33 (2009), 1823-1838

[5] Henke, S., Hamann, T., Grabe, J., 2012. "*Numerische Untersuchungen zur Bodenverdichtung mittels Rütteldruckverfahren* ", 2. Symposium Baugrundverbesserung in der Geotechnik, 13.-14. September 2012, TU Wien

[6] Heins, E., Grabe, J., 2015. "*Numerische Simulation einer Bodenverbesserungsmaßnahme infolge Rütteldruckverdichtung*", In: Numerische Methoden in der Geotechnik, BAW Mitteilungen 98, 59-68

[7] Osinov, V.A., Chrisopoulos, S., Triantafyllidis, T., 2013. "*Numerical Study of the Deformation of Saturated Soil in the Vicinity of a Vibrating Pile*", Acta Geotechnica 8 (2013), 439–446

[8] Osinov, V.A., 2013. "*Application of a High-Cycle Accumulation Model to the Analysis of Soil Liquefaction around a Vibrating Pile Toe*", Acta Geotechnica 8 (2013), 675–684

[9] Niemunis, A., Herle, I., 1997. "*Hypoplastic Model for Cohesionless Soils with Elastic Strain Range*", Mechanics of Cohesive-Frictional Materials, Vol. 2 (1997), 279-299

[10] Niemunis, A., Wichtmann, T., Triantafyllidis, T., 2005. "*A High-Cycle Accumulation Model for Sand*", Computers and Geotechnics, Vol. 32, Issue 4 (June 2005), 245-263

[11] von Wolffersdorff, P.-A., 1996. "*A Hypoplastic Relation for Granular Materials with a Predefined Limit State Surface*", Mechanics of Cohesive-Frictional Materials, Vol. 1 (1996), 251-271

[12] Mašín, D., 2017. "*Plaxis Implementation of Hypoplasticity Including Standalone Abaqus Umat Subroutines*", 12th September 2017 from https://web.natur.cuni.cz/uhigug/masin/plaxumat/

[13] Bakroon, M., Daryaei, R., Aubram, D., Rackwitz, F., 2018. "*Implementation and Validation of an Advanced Hypoplastic Model for Granular Material Behavior*", 15th International LS-DYNA® Users Conference, 10th-12th June 2018 in Detroit, Michigan, USA

[14] Aubram, D., 2019. "*Explicitly Coupled Consolidation Analysis Using Piecewise Constant Pressure*", Acta Geotechnica (2019), https://doi.org/10.1007/s11440-019-00792-z

[15] Lysmer, J., Kuhlemeyer, R., 1969. "*Finite Dynamic Model for Infinite Media*", Journal of the Engineering Mechanics Division, 1969, Vol. 95, Issue 4, 859-878

[16] Denies, N., Canou, J., Roux, J.-N., Holeyman, A., 2014. "*Vibrocompaction Properties of Dry Sand*", Canadian Geotechnical Journal, 51 (2014), 409-419, dx.doi.org/10.1139/cgj-2012-0436

[17] Wichtmann, T. 2016, "*Soil Behaviour under Cyclic Loading – Experimental Observations, Constitutive Description and Applications*", Habilitation thesis, Veröffentlichungen des Institutes für Bodenmechanik und Felsmechanik am Karlsruher Institut für Technologie (KIT), Heft 181, 2016

[18] Belytschko, T., Kam Liu, W., Moran, B., Elkhodary, K. I., 2014. "*Nonlinear Finite Elements for Continua and Structures*" Second Edition, John Wiley & Sons, UK, 804 pages.

[19] Youd, T.L., 1972. "*Compaction of Sands By Repeated Shear Straining*", Journal of the Soil Mechanics and Foundations Division, 1972, Vol. 98, Issue 7, Pg. 709-725